Revista de la Sociedad Geológica de España 27 (1)

ISSN (versión impresa): 0214-2708
ISSN (Internet): 2255-1379

SULFATE ISOTOPE COMPOSITIONS ($\delta^{34}S$, $\delta^{18}O$) AND STRONTIUM ISOTOPIC RATIOS ($^{87}Sr/^{86}Sr$) OF TRIASSIC EVAPORITES IN THE BETIC CORDILLERA (SE SPAIN)

Composiciones isotópicas del sulfato ($\delta^{34}S$, $\delta^{18}O$) y razones isotópicas del estroncio ($^{87}Sr/^{86}Sr$) en evaporitas triásicas de la Cordillera Bética (SE España)

Federico Ortí[1], Alberto Pérez-López[2, 3], Javier García-Veigas[4], Laura Rosell[1], Dionisio I. Cendón[5] and Fernando Pérez-Valera[6]

[1] Departament de Geoquímica, Petrologia i Prospecció Geològica, Universitat de Barcelona, C/ Martí i Franqués, s/n, 08028 Barcelona, Spain
[2] Instituto Andaluz de Ciencias de la Tierra, (CSIC-Universidad de Granada), Avda. de las Palmeras nº4, 18100 Armilla (Granada), Spain
[3] Departamento de Estratigrafía y Paleontología, Facultad de Ciencias, Universidad de Granada, Avda. Fuentenueva, s/n, 18002 Granada, Spain
[4] CCiTUB Centres Científics i Tecnològics, Universitat de Barcelona, C/ Lluís Solé i Sabarís, 1-3, 08028 Barcelona, Spain. garcia_veigas@ub.edu
[5] ANSTO Australian Nuclear Science and Technology Organisation, Kirrawee DC, NSW 2232, Australia
[6] Dpto. de Geología, Facultad de Ciencias Experimentales, Campus de Las Lagunillas s/n. 23071 Jaén, Spain

***Abstract**: Sulfate isotope compositions ($\delta^{34}S$ and $\delta^{18}O$) and strontium isotope ratios ($^{87}Sr/^{86}Sr$) of Triassic evaporites in the Betic Cordillera are addressed for the first time in the present work. Isotope values have been determined in gypsum and anhydrite samples of the Germanic-type facies (Buntsandstein, Muschelkalk and Keuper) coming from different outcrops spanning the complete Triassic Period and corresponding to both the Internal Zones and the External (Prebetic, Subbetic) Zones of this chain. More precise age assignments and stratigraphic controls are often obscured because of the intense halokinetic and tectonic deformation occurred during the Alpine Orogeny in the Betic Cordillera. Isotope values of Triassic sulfates obtained in the present study range between 12.5 and 16.6 ‰ for $\delta^{34}S$, between 8.9 and 16.9 ‰ for $\delta^{18}O$, and between 0.707615 and 0.708114 for $^{87}Sr/^{86}Sr$. These values, as a whole, are in agreement with those of worldwide Triassic marine evaporites.*

***Key words**: Isotopes, sulfate, strontium, evaporites, Triassic, Betic Cordillera.*

***Resumen**: En este trabajo se presenta por primera vez las composiciones isotópicas del sulfato ($\delta^{34}S$ y $\delta^{18}O$) y las relaciones isotópicas del estroncio ($^{87}Sr/^{86}Sr$) en evaporitas triásicas de la Cordillera Bética. Los valores isotópicos han sido determinados en muestras de yeso y anhidrita atribuidas a las facies germánicas (Buntsandstein, Muschelkalk y Keuper) procedentes de diferentes áreas de la cordillera que abarcan el Periodo Triásico completo, y que corresponden tanto a las Zonas Internas (Complejo Alpujárride) como a las Externas (Prebético, Subbético). Debido a la intensa deformación tectónica y halocinética ocurrida durante la Orogenia Alpina en dicha cordillera, es complicado establecer dataciones y controles estratigráficos precisos de las evaporitas triásicas. Los valor isotópicos obtenidos en el presente trabajo varían entre 12,5 y 16,6 ‰ para $\delta^{34}S$, entre 8,9 y 16,9 ‰ para $\delta^{18}O$, y entre 0,707615 y 0,708114 para $^{87}Sr/^{86}Sr$. En conjunto, los valores obtenidos son coincidentes con los asignados en la bibliografía a las evaporitas marinas triásicas a escala global.*

***Palabras clave**: Isótopos, sulfato, estroncio, evaporitas, Triásico, Cordillera Bética.*

Ortí, F., Pérez-López, A., García-Veigas, J., Rosell, L., Cendón, D.I. and Pérez-Valera, F. (2014): Sulfate isotope compositions ($\delta^{34}S$, $\delta^{18}O$) and strontium isotopic ratios ($^{87}Sr/^{86}Sr$) of Triassic evaporites in the Betic Cordillera (SE Spain). *Revista de la Sociedad Geológica de España*, 27(1): 79-89.

The study of the isotope composition of the evaporitic sulfates is one of the most relevant aspects for their geochemical and genetic characterization. The sulfate isotope compositions ($\delta^{34}S$ and $\delta^{18}O$) and the strontium isotope ratios ($^{87}Sr/^{86}Sr$) are the most commonly used geochemical markers to determine the marine or non-marine origin of the mother brines and the contribution of different water types to evaporitic basins. This determination can be done by means of both the age curves of sulfur and oxygen isotopes in seawater sulfate and the age curve of marine strontium isotope ratios, which may also provide guidance on the age of the studied sulfates if it remains unknown. These curves are being continuously verified and worldwide improved (e.g., Claypool et al., 1980; Burke et al., 1982; Korte et al., 2003; Wortmann and Paytan, 2012). The ocean sulfate concentration and its isotope composition have changed over time as a consequence of different processes: 1) continental weathering mainly affecting older evaporites, 2) deposition of sulfur-bearing sediments, mainly evaporites, 3) volcanism and hydrothermal activity, and 4) changes in oceanic water circulation promoting periods of oceanic anoxia and sulfide formation.

When sulfate-bearing minerals precipitate in an evaporitic basin, the $\delta^{34}S_{sulfate}$ and $\delta^{18}O_{sulfate}$ values can be almost coincident with those of the mother brine. Likewise, the $^{87}Sr/^{86}Sr$ ratios of the strontium incorporated (replacing Ca and as co-precipitated celestine inclusions) into these sulfate rocks reflect those of the dissolved Sr^{2+} in brine. Regarding the sulfate isotope compositions, however, the existence of bacterial sulfate reduction activity (BSR) in some evaporitic basins might produce strong isotope fractionation leading to the removal of the isotopically light sulfate and the subsequent enrichment in heavy sulfate isotopes of the residual brine.

The $^{87}Sr/^{86}Sr$ ratio in seawater is considered to be homogeneous due to the large difference between the strontium residence time (several millions of years) and its mixing time (thousands of years) (Holland, 1984). Marine $^{87}Sr/^{86}Sr$ ratios over Earth's history (Burke et al., 1982; Veizer et al., 1999; McArthur et al., 2001) have fluctuated midway between those of radiogenic continental waters ($^{87}Sr/^{86}Sr \sim 0.7110$) and those of hydrothermally altered oceanic basalts ($^{87}Sr/^{86}Sr \sim 0.7030$). Most of the evaporitic basins formed in transitional (marine to non-marine) settings have received different water sources (seawater, runoff, meteoric water, hydrothermal springs, etc.). $^{87}Sr/^{86}Sr$ ratios in each type of water depend on particular chemical water-rock reactions. Strontium isotope ratios in a particular evaporite deposit can be used for deciphering the marine o non-marine origin and for identifying the water sources involved.

The main aim of the present study is to provide an initial compilation of isotope values of Triassic sulfates in the Betic Cordillera in order to know their range of variation and to detect possible differences among the stratigraphic units. The values are compared with those previously reported in other Triassic domains of the Iberian Peninsula. The results obtained may help to interpret the genesis of the Triassic evaporites.

Otherwise, the dissolution of sulfates of preexisting evaporite formations and their reprecipitation in newly-formed ones is a common geologic process that has to be taken into account in order to elucidate the origin of the mother brines. This point is particularly significant in geologic domains containing old evaporite formations suitable to be recycled in younger lacustrine basins affected by intense evaporation.

The Iberian Peninsula is one of the best examples of the scenario outlined above. Thus, Mesozoic and Cenozoic marine evaporite formations (Triassic, lowermost Jurassic, Middle Jurassic, Lower Cretaceous, Upper Cretaceous, Eocene, Upper Miocene) are abundant and occur in the periphery or in the substratum of younger, non-marine evaporitic basins (e.g., basins of Tajo, Ebro, Duero, Calatayud and Teruel, and several Betic basins).

In the Betic Cordillera (Fig. 1), a great number of basins containing evaporite formations were formed during the Neogene in relation with the tectonic evolution of the chain. Some of these formations were marine such as those of Late Messinian age (Sorbas, Níjar and San Miguel de Salinas basins); many others occurred in the transition from marine to non-marine conditions such as those assigned to Late Tortonian–Lower Messinian age (Granada, Lorca, Fortuna and Campo Coy basins); and some others were non-marine (Baza, Las Minas de Hellín basins). As a result of the closure of the Betic seaway during the Late Miocene, a puzzle of interconnected marine sedimentary basins changed their physiographic configuration and evolved to intramontane basins hosting evaporites in most cases. Sulfate and strontium isotope variations in the evaporitic successions of these basins allow to elucidate the time when each basin was closed to the seawater inflow and recycled sulfate from older evaporites.

Thus, another aim of the present study is to supply data which help in understanding the generalized process of evaporite recycling in the Neogene formations of the Betic domain. We hope that our results can be used as a document database of the process.

Triassic evaporite units of the Betic Cordillera

Geological studies of Triassic materials in the Betic Cordillera related to this subject have been recently focused on stratigraphic, sedimentologic, paleogeographic, tectonic, and paleontologic questions (e.g., Flügel et al., 1984; Martín-Algarra et al., 1995; Pérez-Valera and Pérez-López, 2008; Pérez-López and Pérez-Valera, 2012; Pérez-López et al., 2012). The Triassic of the Betic Cordillera shows exten-

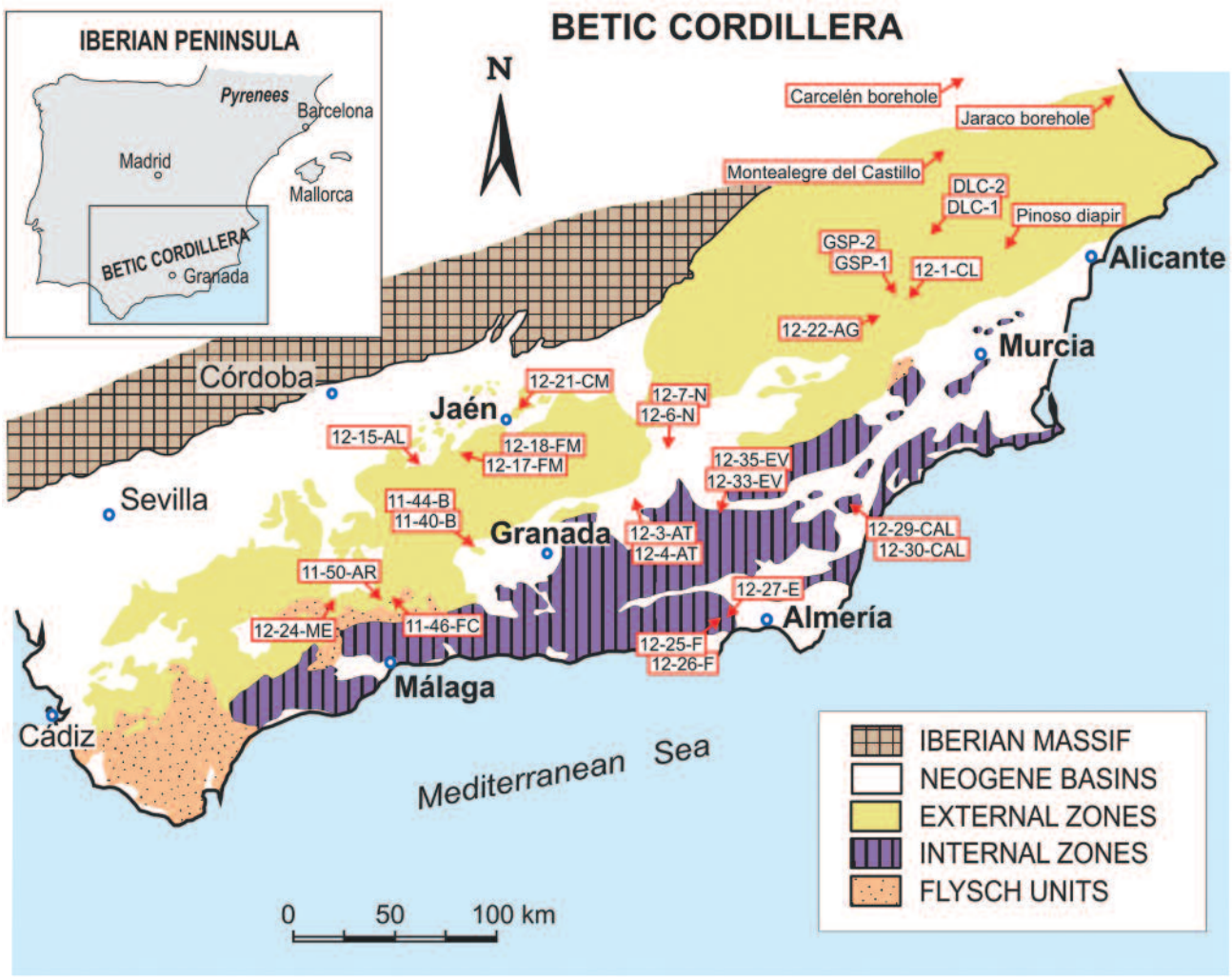

Fig. 1.- Geological sketch map of the main tectonic units in the Betic Cordillera (SE Spain), where the location of the sulfate samples is indicated. Key of the last letters in the sample references: AG, Argos Reservoir; AL, Alcaudete; AR, Archidona; AT, Alicún de las Torres; B, Brácana; CAL, Cuevas del Almanzora; CL, southeast Calasparra; CM, Cerro Molina; DLC, La Celia diapir; E, Énix; EV, El Valle; F, Félix; FC, Fuente Camacho; FM, Fuensanta de Martos; GSP, west Calasparra; ME, Meliones spring; N, Negratín Reservoir.

sive Germanic-type epicontinental facies both in the External Zones and in the Internal Zones, although Alpine facies also occur in the Internal Zones (Pérez-López and Pérez-Valera, 2007) (Fig. 2). However, gypsum deposits are mainly present in the External Zones.

In the outcrops of the External Zones, a number of lithologic units making up the Triassic stratigraphy can be identified (Fig. 3). The older materials, which can be attributed to the Buntsandstein facies, have only been found very locally, in places (SE Calasparra) where red detrital rocks with some gypsum intercalations crop out (Pérez-Valera et al., 2000). The most common facies in the Triassic outcrops are Muschelkalk carbonates (Pérez-Valera and Pérez-López, 2008), gypsum-bearing Keuper facies (Pérez-Valera and Pérez-López, 2008), Norian carbonates of the Zamoranos Formation, and Rhaetian-Lower Jurassic gypsum beds of the Lécera Fm (Gómez and Goy, 1998) correlated with the Carcelén Anhydrite unit of Ortí (1987).

The sulfate beds of these units (secondary gypsum in outcrops, anhydrite at depth) may alternate with halite intervals. Rock salt deposits, up to several hundred metres in thickness, have been recorded in deep wells (Meliones borehole, Table 1) and diapirs (Pinoso and La Rosa diapirs, near Jumilla; mining boreholes in the Pinoso diapir) (Ortí and Pueyo, 1983; Ortí et al., 1996; Pérez-López and Pérez-Valera, 2003). Mechanical contacts, faulting, and brecciation predominate in some of the Triassic outcrops because intense tectonic and halokinetic deformation occurred during the Alpine Orogeny (Pérez-López and Pérez-Valera, 2003). This deformation results in a variety of 'brecciated gypsum units' and 'brecciated outcrops' that are difficult to correlate one to another.

In the three superposed tectonic complexes of the Internal Zones (Nevadofilábride, Alpujárride and Maláguide complexes; Vera, 2004), gypsum beds are only important in the Alpujárride Complex (eastern sector of the chain) (Figs. 1 and 2).

Concerning the Triassic evaporites of the Betic Cordillera, few data on their isotope composition had been published until now. Accordingly, new determinations were carried out for the present paper with the aim to improve the genetic interpretations of these evaporites (Fig. 3).

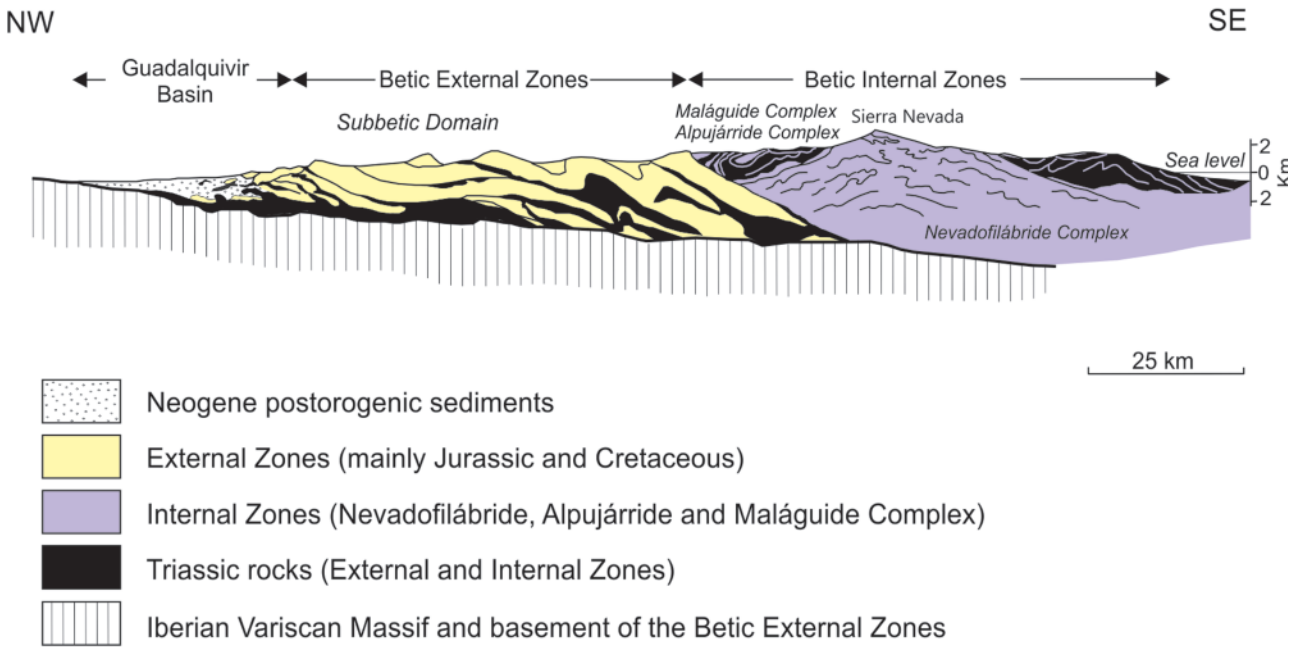

Fig. 2.- Regional cross-section (NW-SE) showing the structure of the Betic Cordillera (Pérez-López and Pérez-Valera, 2007, modified from Vera, 2004). The Triassic deposits constitute, in general, the main detachment level of the tectonic units. Triassic outcropping occurs in a notably disrupted and fractured manner, and sometimes displays a mixture of different tectonic units. In this context, the presence of 'brecciated gypsum units' is frequent due to tectonism and diapirism.

Materials and methods

Appropriate outcrops were selected in order to have a good representation of the most significant Triassic gypsum units of the External (Prebetic, Subbetic) Zones, including the 'brecciated gypsum unit/facies', and of the Internal Zones. Triassic units sampled in the External Zones mainly correspond to gypsum beds of the Jaén Keuper Group (Pérez-Lopez, 1998), especially of its upper part (Tables 1 and 2). However, we have also sampled gypsum associated with Anisian detrital rocks (Buntsandstein facies), Ladinian carbonates (Muschelkalk facies) of the Cehegín Formation, and gypsum beds that overly the Norian carbonates of the Zamoranos Formation. In the Internal Zones, sampling was completed with a number of Triassic rocks of the Alpujárride Complex.

Mineralogical identification of 20 samples collected from all these Triassic outcrops of the Betic Cordillera (Fig. 1, Tables 1 and 2) was carried out by X-Ray Diffraction and by Scanning Electron Microscopy. Thin sections of 15 representative samples were prepared for petrographic characterization.

Secondary gypsum and anhydrite samples (16 and 3, respectively) were selected for sulfate isotope analyses (Table 2). Each sample was dissolved in distilled water, acidified to pH 3 adding HCl and then reprecipitated as barium sulfate by means of a solution of $BaCl_2$. Sulfur and oxygen isotope compositions were analyzed by the on-line method. The $\delta^{34}S_{V\text{-}CDT}$ was determined with a Carlo Erba 1108 Elemental Analyzer and the $\delta^{18}O_{V\text{-}SMOW}$ with a TC-EA unit, both coupled to an IRMS Thermo Finnigan Delta Plus XP at the Stable Isotope Laboratory of the CCiTUB (*Universitat de Barcelona*). The obtained $\delta^{34}S$ and $\delta^{18}O$ values (Table 2) are reported in ‰ relative to the Vienna Canyon Diablo Troilite (V-CDT) standard for sulfur and to the Vienna SMOW standard for oxygen. The analytical error (2σ) was ± 0.2 ‰ for $\delta^{34}S$ and ± 0.4 ‰ for $\delta^{18}O$. Isotope compositions obtained by the Standard NBS-127 were of 20.3 ± 0.1 ‰ for $\delta^{34}S$, and of 9.3 ± 0.2 ‰ for $\delta^{18}O$.

Strontium isotope ratios ($^{87}Sr/^{86}Sr$) were determined in 9 samples of powdered gypsum (Table 2) containing trace amounts of celestine, dolomite and/or magnesite, and in one anhydrite sample. All the samples were dissolved in 2 mL of >18 $M\Omega cm^{-1}$ water in order to minimize the dissolution of dolomite and leaching of Sr from clays and other terrigenous material. Samples were left to react overnight and then centrifuged. The supernatant was removed, taking care not to disturb any undissolved residue. The supernatant was dried, redissolved in HNO_3, loaded onto Sr-Spec resin pre-conditioned columns and the eluted Sr was finally loaded onto a Ta filament with H_2O and H_3PO_4, for TIMS (Thermal Ionisation Mass Spectrometry) analysis. The isotopic ratios were measured on a VG 354 TIMS with a long term analytical precision of ± 0.000014 measured on NBS-987 ($^{87}Sr/^{86}Sr$: 0.710288 ± 0.000014). $^{87}Sr/^{86}Sr$ ratios were normalized to $^{86}Sr/^{88}Sr = 0.1194$.

Results

Mineralogy and petrology

Mineral composition of sulfate samples of the Betic Triassic selected for the present work is relatively homogeneous (Tables 1 and 2). Predominant sulfate is gypsum, with minor amounts of celestine, which is present in all samples, and anhydrite in some samples. Associated carbonates are mainly dolomite, with minor calcite and scarce magnesite. Accessory minerals are quartz, hematite and

EXTERNAL ZONES			
Sample	**Location**	***Rock type and macroscopic features***	***Texture and host material***
11-40-B	Quarry located to the N of the Puente Castilla bridge; to the S of Brácana village; Granada basin	Secondary gypsum rock. Light-coloured, fine-grained, laminated gypsum clast with little host material, which is embedded in a gypsum breccia	Gypsum texture derived from the hydration of a precursor anhydrite rock. Gypsum components: complex net of veins, which show the same optical extinction in wide parts of the thin section; satin spar (fibrous) veins; microcrystalline groundmass; some euhedral crystals. Small celestine crystals, with intensely corroded boundaries. The host material is formed by: scattered, anhedral/subhedral crystals of dolomite (?); and few euhedral quartz crystals
11-46-FC	Quarry located to the N of Fuente Camacho village; near Archidona town, to the W of Granada	Secondary gypsum rock. Light-coloured, with diffuse banding; the sample is a pure gypsum block of alabastrine appearance, which is included in a gypsiferous breccia	Gypsum texture derived from the hydration of a precursor anhydrite rock; the texture is party recrystallized. Gypsum components: large (variable sizes between 0.5 and 1 mm), euhedral (prismatic sections) crystals, relatively oriented, with somewhat undulose optical extinction, and without anhydrite relics. Small, isolated celestine crystals. The very scarce host material is formed by: microcrystals and coarser crystals of dolomite that seem to replace gypsum
12-3-AT	Alicún de las Torres village; to the N of Guadix town (Guadix basin); Granada province	Secondary gypsum rock. Banded gypsum with dark, porphyroblastic laminae, and some fine-grained, light-coloured laminae	Mixed, heterometric gypsum texture derived from the hydration of a precursor anhydrite rock, with the appearance of partial recrystallization. Gypsum components: porphyroblasts, microcrystalline groundmass, and euhedral crystals. Porphyroblasts vary from isolated crystals to radial aggregates with undulose extinction and planar boundaries, and all they retain small anhydrite inclusions and seem to be partly recrystallized. Celestine crystals, up to 1 mm in size, are present; they have corroded boundaries and contain small anhydrite inclusions. The host material is formed by dolomicrite matrix and some dolomicritic clasts scattered throughout the thin section giving way to a diffuse lamination
12-17-FM	Fuentesanta de Martos village; Jaén province; upper part of K3 unit	Secondary gypsum rock. Nodule of pink, microcrystalline gypsum including some grey carbonate matrix, and sourrounded by red clay	Mixed, heterometric gypsum texture derived from the hydration of a precursor anhydrite rock, with the appearance of partial recrystallization. Gypsum components (all they without anhydrite relics): unoriented, euhedral to subhedral crystals; some veins; microcrystalline groundmass; large crystalline plates with undulose extinction. Small, scattered celestine crystals. The host material is formed by: rectangular clasts of phyllosilicate rocks; scattered, anhedral dolomite crystals; and few crystals of authigenic quartz bearing tiny inclusions of anhydrite and gypsum
DLC-1	La Celia diapir; Murcia province; Keuper	Secondary gypsum rock. Light-coloured, laminated gypsum	Mixed, heterometric gypsum texture derived from the hydration of a precursor anhydrite rock. Gypsum components: large porphyroblastic plates; fine-grained alabastrine masses; very irregular veins. The porphyroblastic plates have undulose extiction and sutured contacts; they are poikilitic locally and contain relic inclusions of anhydrite. The host material is formed by: abundant micrite arranged in thin, diffuse laminae; possible pseudomorphs of precursor microselenite crystals forming laminae; aggregates of sparitic, dark crystals of possible dolomite; hematite crystals (20 to 60 μm in size)
DLC-2	La Celia diapir; Murcia province; Keuper	Secondary gypsum rock. White gypsum formed by large crystals	Porphyroblastic gypsum texture derived from the hydration of a precursor anhydrite rock. Gypsum components: porphyroblasts with the appearance of large, crystalline plates; these plates are anhedral, have irregular extinction and euhedral interlocking boundaries, and bear abundant anhydrite relics. The host material is almost lacking: some scattered micrite; few residual masses of spherulites (zeolites?)
INTERNAL ZONES			
Sample	**Location**	***Rock type and macroscopic features***	***Texture and host material***
12-25-F	To the SE of Félix village; Almería province; Alpujárride Complex	Secondary gypsum rock (clast associated with the brecciated matrix in the sample 12-26F). Light grey, medium-grained, laminated gypsum with millimetre-sized crystals	Heterometric, recrystallized gypsum texture derived from the hydration of a precursor anhydrite rock. Gypsum components: coarse (up to 1 mm in size), unoriented, euhedral-to-subhedral crystals with planar to interlocking boundaries, without anhydrite inclusions; some microcrystalline matrix. Small celestine crystals. The scarce host material is formed by: dolomite (microsparite to sparite) arranged in diffuse laminae
12-26-F	To the SE of Félix village; Almería province; Alpujárride Complex	Detrital rock; microbrecciated gypsiferous matrix. Grey and yellow tonalities, with an arenite/wacke appearance	Calcareous microbreccia with heterometric-sized (silt, sand and granule) clasts. Components: clasts of carbonates (dolostone, micritic rocks), phyllosilicates and sandstones (quartz-arenites); isolated crystals of dolomite and quartz; gypsum cement formed by large, anhedral, poikilitic gypsum crystals; 'hexagonal' crystals of pyrite; tiny crystals of celestine; tiny magnesite crystals that are included within the dolomite clasts; abundant gypsum cementing preexisting porosity

Table 1.- Petrography of representative calcium sulfate samples of the Triassic outcrops in the Betic Cordillera.

INTERNAL ZONES			
Sample	**Location**	***Rock type and macroscopic features***	***Texture and host material***
12-27-E	To the SW of Enix village; Almería province; Alpujárride Complex	Gypsiferous dolostone, with the appearance of a grey, laminated gypsum rock	Irregular distribution of dolomite crystals and dolostone (?) clasts arranged in diffuse lamination, in association with abundant gypsum crystals. Components: anhedral, dirty carbonate crystals; coarse, euhedral to subhedral gypsum crystals often with undulose extinction, which poikilitically include carbonate crystals and clasts, to which they replace locally. These gypsum crystals, which have not anhydrite relics, behave as a cement with an anhedral-to-blocky texture; tiny celestine and pyrite crystals; clasts of quartz-arenites; clasts of other siliceous rocks and particles
12-29-CAL	Quarry in the Sierra de Almagro, to the N of Cuevas de Almanzora village; Almería province, Alpujárride Complex	Secondary gypsum rock. Massive bed of white, sacaroid (medium-grained) gypsum	Dense, recrystallized gypsum texture, which originally was derived from the hydration of a precursor anhydrite rock. Gypsum components: euhedral (prismatic sections) and subhedral, unoriented gypsum crystals with variable size (up to 1 mm) and without anhydrite relics, whose boundaries are from planar (blocky texture) to sutured; and very scarce gypsum groundmass. Relatively large celestine crystals are present, which appear to be corroded by gypsum. The host material is formed by scattered, anhedral to subhedral dolomite crystals
12-30-CAL	Quarry in the Sierra de Almagro, to the N of Cuevas de Almanzora village; Almería province; Alpujárride Complex	Gypsiferous (gypsum veins) dolostone, with the appearance of light-coloured, massive, very pure marble or alabaster rock	Microsparitic-to-sparitic, xenotopic dolostone formed by heterometric dolomite crystals arranged in diffuse lamination. A vein system formed by transparent, euhedral (prismatic sections) to subhedral gypsum crystals is present; these crystals behave as a cement and have not anhydrite inclusions. Those parts of the dolostone in close relation with the gypsum veins display coarse dolomite crystals, which in turn are associated with coarse gypsum crystals; many other parts of the rock show gypsum crystals isolated or forming small clusters; all these parts probably represent preexisting porosity which was later cemented by gypsum and large dolomite crystals. Some celestine and quartz crystals are present as well as prismatic crystals of Na-silicate (with almost straight optical extinction, and with several types of twins)

Table 1.- (continuation) Petrography of representative calcium sulfate samples of the Triassic outcrops in the Betic Cordillera.

clays (clay mineralogy was not identified in the present work).

The petrographic study of selected thin sections is summarized in Table 1. Gypsum is secondary (derived from the hydration of precursor anhydrite) in all the samples, and its textures vary largely from unaltered to strongly recrystallized.

Non-recrystallized gypsum textures are only present in some samples of the External Zones. These little modified textures show a number of petrographic components, some of them preserving anhydrite relics: porphyroblastic crystals, either isolated or in groups; microcrystalline groundmass (alabastrine matrix); euhedral to subhedral crystals, in which prismatic sections are predominant; large crystalline plates with contact boundaries ranging from planar to interpenetrated; and fibrous (satin spar) veins. Many gypsum textures combine several of these components. Recrystallized textures are evidenced by progressive changes from these components to a homogeneous texture formed by coarse, euhedral crystals either aligned or unoriented, in which anhydrite relics are totally absent. These recrystallized textures are preferentially observed in samples of the Internal Zones, given the metamorphism they have undergone.

Carbonate associated with secondary gypsum is mainly dolomite, either forming discontinuous laminae or as irregularly distributed masses within the rock. Anhydrite samples coming from boreholes show a marked recrystallized texture, which is formed by coarse crystals with interpenetrated contact boundaries.

The celestine crystals in the gypsum samples have variable size, from tens of μm up to1 mm. The growth timing of these crystals is not readily determined. Presently, small amounts of celestine precipitate in association with gypsum in both marine and non-marine modern evaporite environments. In some of the studied samples celestine might have been late diagenetic given that they contain tiny inclusions of anhydrite, which in most cases was a burial (late) diagenetic product. In general, the celestine crystals exhibit boundaries that are corroded by the hosting secondary gypsum, suggesting that celestine was affected by (was formed prior to) the final hydration of anhydrite into secondary gypsum. Whatever the case, the abundance of celestine is very low. Presumably, such a low content and the low solubility of $SrSO_4$ suggest that celestine has no influence on the strontium isotope determination.

Sulfate isotope compositions ($\delta^{34}S$, $\delta^{18}O$) and strontium isotope ratios ($^{87}Sr/^{86}Sr$)

Sulfur isotope compositions ($\delta^{34}S_{sulfate}$) of Triassic evaporites of the Betic Cordillera determined in the present study range between 12.5 and 16.6 ‰ averaging 14.9 ± 1.0 ‰. The corresponding oxygen isotope compositions ($\delta^{18}O_{sulfate}$) exhibit a wider range, from 8.9 to 16.9 ‰ with an average value of 12.6 ± 2.1 ‰ (Table 2). Strontium isotope counterparts range between 0.707615 and 0.708114 (Table 2).

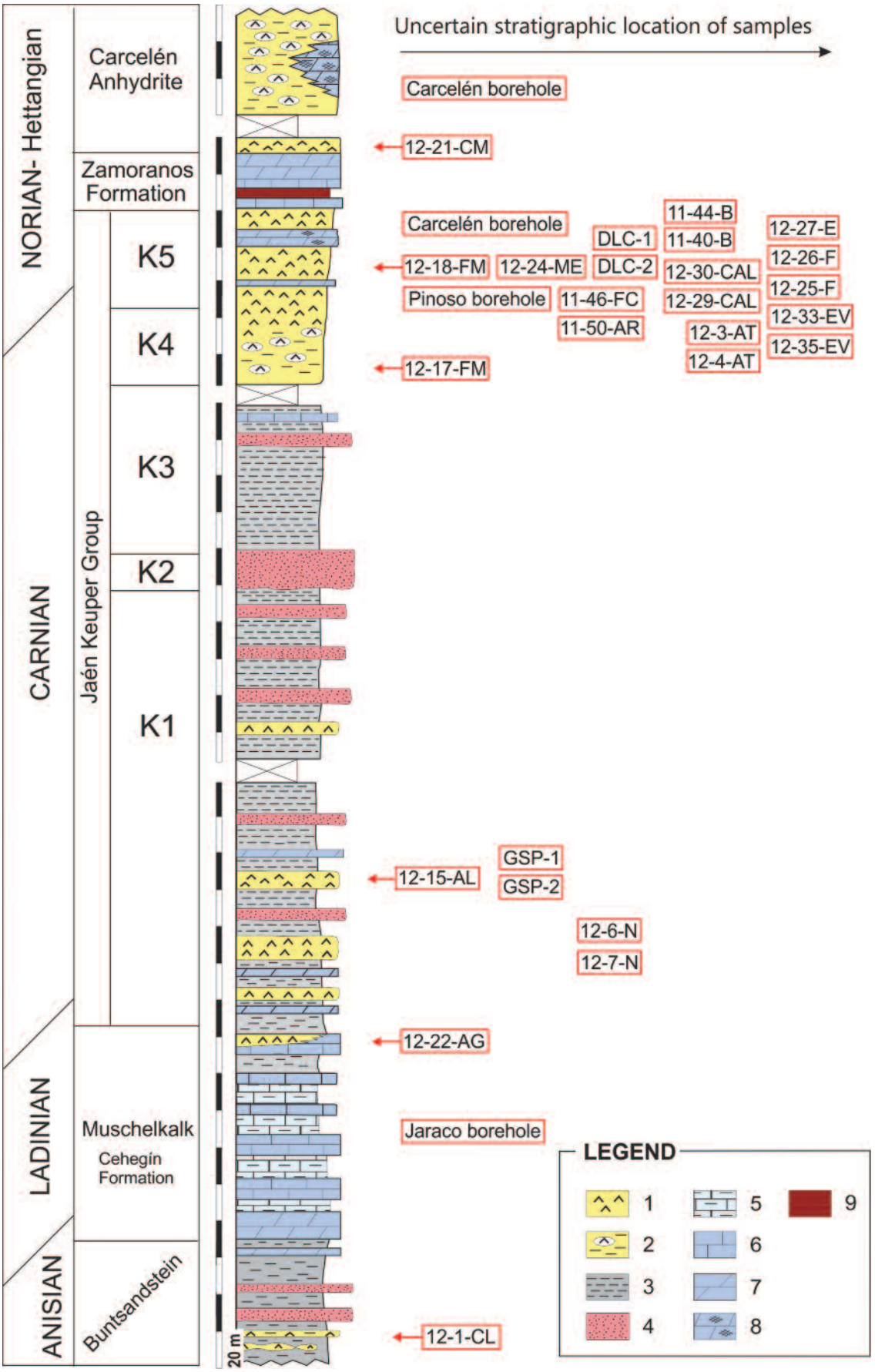

Fig. 3.- Triassic stratigraphy in the Betic External Zones (modified from Pérez-López, 1998), where the units hosting evaporites are shown and the situation of the sulfate samples is indicated. These evaporites contain associated deposits of anhydrite and salt, which are known from boreholes. Legend: 1: Gypsum/anhydrite 2: Nodular gypsum and clay; 3: Lutite/marl; 4: Sandstone; 5 Marly limestone and marl 6: Limestone; 7: Dolostone; 8: Carniolar carbonate 9: Red claystone and conglomerate. Schema out of scale.

BETIC EXTERNAL ZONES									
Age range	**Sample**	**Coordinate**	**Location (Province[1])**	**$\delta^{34}S$‰**	**$\delta^{18}O$‰**	**$^{87}Sr/^{86}Sr$**	**Lithofacies/(unit)**	**Mineralogy[2]**	**Ref.[3]**
Upper Triassic?	11-40-B	37º 12' 15'' 03º 56' 25''	S Brácana (GR)	14.0	12.1		Laminated secondary gypsum (brecciated units)	gyp (cel, q)	a
Upper Triassic?	11-44-B	37º 12' 05'' 03º 56' 29''	S Brácana (GR)	13.6	11.8		Alabastrine secondary gypsum (brecciated units)	gyp (cel, q)	a
Norian?	11-46-FC	37º 06' 18'' 04º 16' 04''	N Fuente Camacho (GR)	15.4	12.8		Alabastrine secondary gypsum (Keuper, K5 unit?)	gyp (cel, dol, cal)	a
Norian?	11-50-AR	37º 04' 56'' 04º 22' 31''	S Archidona (MA)	14.5	11.5		Alabastrine secondary gypsum (Keuper, K5 unit?)	anh (dol, gyp)	a
Anisian	12-1-CL	38º 12' 22'' 01º 38' 10''	SE Calasparra (MU)	14.7	13.7	0.708114	Nodular secondary gypsum (Bunt-sandstein)	gyp (q, anh, cel)	*
Upper Triassic?	12-3-AT	37º 29' 17'' 03º 08' 03''	Alicún de las Torres (GR)	15.0	11.6	0.707615	Laminated secondary gypsum block	gyp, cel	*
Upper Triassic?	12-4-AT	37º 29' 18'' 03º 08' 03''	Alicún de las Torres (GR)	15.8	16.7	0.707896	Laminated secondary gypsum (brecciated units)	gyp (mgs, cel)	*
Carnian-Norian	12-6-N	37º 33' 51'' 2º 57' 35''	N Bácor (GR)	15.2	11.2	0.707857	Laminated secondary gypsum (Keuper)	gyp (anh, dol, mgs, cel)	*
Carnian-Norian	12-7-N	37º 33' 51'' 2º 57' 34''	N Bácor (GR)	15.6	13.5		Laminated secondary gypsum (Keuper)	gyp, cel	*
Carnian	12-15-AL	37º 35' 13'' 04º 09' 06''	W Alcaudete (J)	16.2	12.3		Laminated secondary gypsum (Keuper, K1 unit)	gyp (anh, dol, cel)	*
Carnian-Norian	12-6-N	37º 33' 51'' 2º 57' 35''	N Bácor (GR)	15.2	11.2		Laminated secondary gypsum (Keuper)	gyp (anh, dol, mgs, cel)	*
Carnian-Norian	12-7-N	37º 33' 51'' 2º 57' 34''	N Bácor (GR)	15.6	13.5		Laminated secondary gypsum (Keuper)	gyp, cel	*
Norian	12-18-FM	37º 38' 24'' 03º 55' 06''	Fuensanta de Martos (J)	15.4	16.9		Laminated secondary gypsum (K5 unit)	gyp, cel	*
Rhaetian	12-21-CM	37º 48' 09'' 03º 44' 11''	Puente Tablas (J)	14.8	10.0	0.707757	Laminated secondary gypsum (Carcelén Anhydrite unit)	gyp (anh, dol, cel)	*
Ladinian-Carnian	12-22-AG	38º 10' 15'' 01º 43' 24''	Argos (MU)	16.4	13.5	0.707720	Laminated gypsum (uppermost part of Muschelkalk)	gyp, cel	*
Upper Triassic?	12-24-ME	36º 59' 13'' 04º 44' 50'	W Antequera Meliones borehole (MA)	14.8	13.6	0.707985	Anhydrite core (923 m depth)	anh, dol (q, mgs, cel)	*
Carnian	DLC-1	38º 26' 25.3'' 01º 32' 10.5'	La Celia diapir (MU)	14.5	10.7		Laminated secondary gypsum (Keuper)	gyp (anh, cal, cel, q, hem, mgt)	*
Carnian	DLC-2	38º 26' 25.3'' 01º 32' 10.5'	La Celia diapir (MU)	14.6	10.8		Megacrystalline secondary gypsum (Keuper)	gyp (anh, mgt)	*
Upper Triassic	GSP-1	38º 13' 45'' 01º 42' 47''	Calasparra (MU)	15.4	14.6		Laminated secondary gypsum (Keuper)	Gyp	b
Upper Triassic	GSP-2	38º 13' 45'' 01º 42' 47''	Calasparra (MU)	13.8	12.4		Laminated secondary gypsum (Keuper)	Gyp	b
Upper Triassic			Montealegre del Castillo (ALB)	13.8			Laminated secondary gypsum (Keuper)	Gyp	d
Upper Triassic	S2-168.3 m	38º 23' 31'' 01º 1' 30''	Pinoso diapir borehole (ALI)	12.5	11.5		Laminated anhydrite (Keuper)	Anh	c
Upper Triassic	S2-318.8 m	38º 23' 31'' 01º 1' 30''	Pinoso diapir borehole (ALI)	15.8	10.9		Laminated anhydrite (Keuper)	Anh	c
Rhaetian-lower-most Jurassic	1242 m	39º 5' 16.60'' 01º 18' 12.70''	Carcelén borehole (ALB)	16.3	12.6		Nodular anhydrite (Anhydrite Zone)	Anh	c
Rhaetian-lower-most Jurassic	1247 m	39º 5' 16.60'' 01º 18' 12.70''	Carcelén borehole (ALB)	14.8	13.9		Nodular anhydrite (Anhydrite Zone)	Anh	c
Rhaetian-lower-most Jurassic	1522 m	39º 5' 16.60'' 01º 18' 12.70''	Carcelén borehole (ALB)	14.8	9.7		Massive anhydrite (Anhydrite Zone)	Anh	c
Rhaetian-lower-most Jurassic	1525 m	39º 5' 16.60'' 01º 18' 12.70''	Carcelén borehole (ALB)	13.3	10.2		Nodular anhydrite (Anhydrite Zone)	Anh	c
Upper Triassic	1948 m	39º 5' 16.60'' 01º 18' 12.70''	Carcelén borehole (ALB)	13.9	8.9		Massive anhydrite (Keuper)	Anh	c
Upper Triassic	1949 m	39º 5' 16.60'' 01º 18' 12.70''	Carcelén borehole (ALB)	13.5	9.0		Massive anhydrite (Keuper)	Anh	c
Middle Triassic	1184.8 m	39º 1' 37.5'' 0º 14' 25.7''	Jaraco-1 borehole(V)	16.6	11.5		Nodular anhydrite (Muschelkalk)	Anh	c
BETIC INTERNAL ZONES									
Age range	**Sample**	**Coordinate**	**Location (Province)**	**$\delta^{34}S$‰**	**$\delta^{18}O$‰**	**$^{87}Sr/^{86}Sr$**	**Lithofacies/(unit)**	**Mineralogy**	**Ref.**
Upper Triassic?	12-25-F	36º 52' 10'' 02º 38' 38''	SE Félix (AL)	15.9	14.9		Secondary gypsum block (brecciated unit, Alpujárride Complex)	gyp (cel, dol, anh) cal, q	*
Upper Triassic?	12-26-F	36º 52' 10'' 02º 38' 38''	SE Félix (AL)	15.8	16.1		Secondary gypsum matrix (brecciated unit, Alpujárride Complex)	gyp (q, dol, pyr) ru, cel, mgs, mus, chl	*
Upper Triassic?	12-27-E	36º 52' 26'' 02º 37' 16''	SW Enix (AL)	16.0	16.3		Laminated grey, secondary gypsum bed (Alpujárride Complex)	gyp (dol, cel) q, mus	*
Upper Triassic?	12-29-CAL	37º 21' 29'' 01º 52' 38''	Cuevas del Almanzora (AL)	15.4	14.2	0.707744	Sacaroid white, secondary gypsum bed (Alpujárride Complex)	gyp (dol, cel) Q, anh?, pyr?	*
Upper Triassic?	12-30-CAL	37º 21' 29'' 01º 52' 38''	Cuevas del Almanzora (AL)	15.1	14.3		Crystalline, secondary gypsum bed (Alpujárride Complex)	dol (gypsum veins) mus	*
Upper Triassic?	12-33-EV	37º 19' 20'' 02º 34' 28''	El Valle (AL)	15.2	12.1	0.707819	Crystalline, secondary gypsum block (Nevadofilábride Complex)	anh (gyp, q, mgs, cel)	*
Upper Triassic?	12-35-EV	37º 19' 20'' 02º 34' 28''	El Valle (AL)	15.4	10.8		Crystalline, anhydrite rock (Nevadofilábride Complex)	anh (mgs, cel, dol)	*

[1] **Province:** AL Almería, ALB Albacete, ALI Alicante, GR Granada, J Jaén, MA Málaga, MU Murcia, V Valencia
[2] **Mineralogy:** anh anhydrite, cal calcite, cel celestine, chl chlorite, dol dolomite, hem hematite, mgs magnesite, mgt magnetite, mus muscovite, pyr pyrite, q quartz, ru rutile
[3] **Ref.** Reference: [a] García-Veigas *et al*. (2013); [b] Gibert *et al*. (2007); [c] Utrilla *et al*. (1992); [d] Gómez Alday *et al*. (2004); *: this work.

Table 2.- Location, isotope values ($\delta^{34}S$ and $\delta^{18}O$ of sulfate; $^{87}Sr/^{86}Sr$ ratios), and main features of the studied sulfate samples. Province key: AL, Almería; ALB, Albacete; ALI, Alicante; GR, Granada; J, Jaén; MA, Málaga; MU, Murcia; V, Valencia. Data from the present work (*) and from the literature (a, b, c).

Discussion

Besides the former determinations, other isotopic values ($\delta^{34}S_{sulfate}$, $\delta^{18}O_{sulfate}$) available in the literature (Utrilla et al., 1992; Gómez-Alday et al., 2004; Gibert et al., 2007, García-Veigas et al., 2013) of Triassic sulfates coming from the central and eastern sectors of the Betic Cordillera (Pinoso diapir and Montealegre del Castillo outcrops, Carcelén and Jaraco-1 boreholes; Calasparra outcrops; outcrops in surrounding areas of the Granada basin) are included in Tables 1 and 2. Thus, values ranging from 12.5 to 17 ‰ for $\delta^{34}S$ and from 9 to 17 ‰ for $\delta^{18}O$ are the most commonly found in the Triassic evaporites of the Betic domain (Fig. 4). As a whole, these sulfur and oxygen isotope values are similar to those reported for the northwestern domain of the Iberian Range (Alonso-Azcárate et al., 2006; Iribar and Ábalos, 2011) and for the Catalan Coastal Ranges and the Pyrenean Chain (Utrilla et al., 1992). All these results are also similar to the values referred to in the literature for marine Triassic sulfates (Claypool et al., 1980; Cortecci et al., 1981; Rick, 1990; Fanlo and Ayora, 1998; Longinelli and Flora, 2007; Boschetti et al., 2011). The only sample analysed assigned to the Buntsandstein facies is in the range of the Keuper values. The two samples assigned to the Muschelkalk facies show higher $\delta^{34}S$ values, close to 16.5 ‰, while the corresponding $\delta^{18}O$ data fit well with the Triassic range.

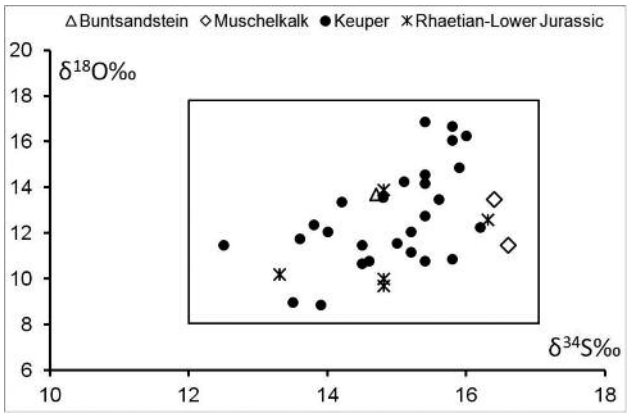

Fig. 4.- Plot of the sulfate isotope composition ($\delta^{34}S$ *vs* $\delta^{18}O$) of the studied samples.

The $^{87}Sr/^{86}Sr$ variations for the Phanerozoic marine sedimentary rocks (Burke et al., 1982; Veizer et al., 1999; Korte et al., 2003) record a marked increase from values close to 0.706900 during the Late Permian to 0.708200 at the end of the Early Triassic. A progressive drop occurs during the Middle Triassic to values close to 0.707600 at the end of the Ladinian stage, although some small different trends have been reported between the Tethys and the mid-European Muschelkalk Sea values (Korte et al., 2003). Most of the Late Triassic time period, to which the Keuper facies corresponds, is characterized by a progressive radiogenic enrichment with a $^{87}Sr/^{86}Sr$ trend from 0.707600 to 0.707800 followed by a one-off increase to ~ 0.708200 at the end of the Norian stage, and a final drop to ~ 0.707800 during the Rhaetian stage. Strontium isotope data from the Betic evaporites in the present study are in the range with those expected for Triassic marine evaporites (Fig. 5). The sample assigned to the Buntsandstein facies shows the highest ratio (sample 12-1-CL; $^{87}Sr/^{86}Sr$: 0.708114; Tables 1 and 2) while the sample attributed to the uppermost part of the Muschelkalk carbonates (sample 12-22-AG; $^{87}Sr/^{86}Sr$: 0.707720; Tables 1 and 2) falls within the general Triassic range. Significant isotopic differences were not observed between samples from the External Zones and the Internal Zones (Fig. 6).

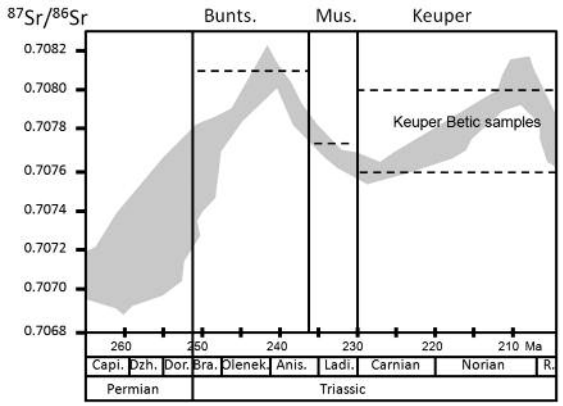

Fig. 5.- $^{87}Sr/^{86}Sr$ variations for the Permian-Triassic marine sedimentary rocks (after Burke et al., 1982, Veizer et al., 1999, and Korte et al., 2003), with indication of the $^{87}Sr/^{86}Sr$ values of the studied samples (dotted lines in the Buntsandstein and Muschelkalk samples; area comprised between dotted lines in the Keuper samples).

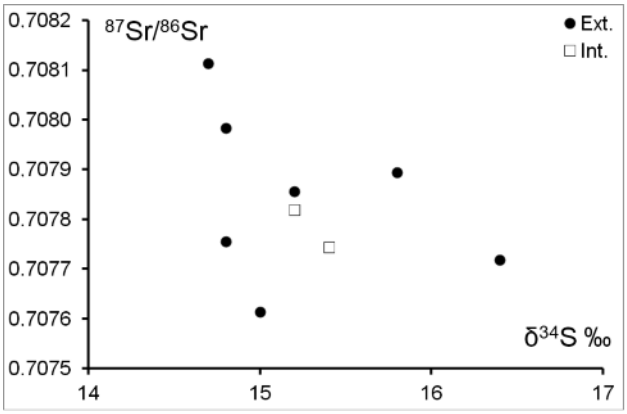

Fig. 6.- Plot of the $^{87}Sr/^{86}Sr$ *vs* $\delta^{34}S$ values of the studied samples. Ext.: External Zones; Int.: Internal Zones.

Strontium isotope ratios reported for Keuper evaporites of the Cameros Basin, in the Northern sector of the Iberian Range (Alonso-Azcárate et al., 2006), are within the lower part of the range obtained in the present work (0.707615 – 0.708114).

A brief reference can be made to the interest of these data regarding the origin of the Neogene evaporite formations in the Betic domain. Two factors should be considered: (1) the chemical recycling of Triassic sulfates into the Neogene ones, and (2) the nature of the mother brines from which the Neogene evaporites precipitated.

Thus, some of the Neogene evaporites have sulfates characterized by $\delta^{34}S$ values suggesting direct recycling of Triassic sulfates in meteoric waters (14-16 ‰) as well as progressively higher values (up to 20-21 ‰) interpreted as derived from several stages of recycling of the Triassic sulfates in the Baza basin (Gibert et al., 2007). Other Neogene evaporites show increasing $\delta^{34}S$ values from the base (20-22 ‰) to the top (near 16-17 ‰) indicating a change in the mother brines from initially marine (as demonstrated by other geochemical indicators also) to isotopically depleted, non-marine waters, in which dissolved sulfate probably comes from the recycling of Triassic evaporites to the top. In this group, the evaporite units of the Granada basin (García-Veigas et al., 2013) and some of the evaporite units of the Lorca and Fortuna basins (Playà et al., 2000) are included. Other Neogene evaporites show intermediate $\delta^{34}S$ values (14-19 ‰) suggesting continuous mixing of marine and meteoric water, as in the Las Minas-Camarillas basin (Hellín Gypsum unit; Moragas et al., 2011).

Conclusions

1) The isotope values of Triassic sulfates of the Betic Cordillera obtained in the present study range between 12.5 and 16.6 ‰ for $\delta^{34}S$, between 8.9 and 16.9 ‰ for $\delta^{18}O$, and between 0.707615 and 0.708114 for $^{87}Sr/^{86}Sr$. These values confirm the marine origin of the Triassic evaporite formations in this geological domain.

2) Significant isotopic differences were not observed between sulfates from the External Zones and the Internal Zones, although the number of samples studied in the Internal Zones was much lower than in the External Zones.

3) The isotopic data of the Triassic sulfates can contribute to a better understanding of the origin, either marine or recycled from older formations, of the Neogene evaporites in the Betic domain.

Acknowledgements

This study was supported by projects CGL2009-11096, CGL2011-24408, CGL2012-33281 of the Spanish Government (*Ministerio de Ciencia e Innovación*), project 2009SGR1451 of the Catalan Government (*Departament d'Innovació, Universitats i Empresa*) and project P08-RNM-03715 of the *Junta de Andalucía*. The authors are indebted to Jordi Illa (GPPG-UB), and to Rosa María Marimón and Eva Aracil (CCiTUB) for their technical support. We thank the reviewers Alfredo Arche and Josep M. Salvany for suggestions and improvements of the original manuscript.

References

Alonso-Azcárate, J., Bottrell, S.H. and Mas, J.R. (2006): Synsedimentary versus metamorphic control of S, O and Sr isotopic compositions in gypsum evaporites from the Cameros Basin. Spain. *Chemical Geology,* 234: 46-57.

Boschetti, T., Cortecci, G., Toscani, L. and Iacumin, P. (2011): Sulfur and oxygen isotope compositions of Upper Triassic sulfates from northern Apennines (Italy): paleogeographic and hydrochemical implications. *Geologica Acta,* 9: 129-147.

Burke, W.H., Denison, R.E., Hetherington, E.A., Koepnick, R.B., Nelson, H.F. and Otto, J.B. (1982): Variation of seawater $^{87}Sr/^{86}Sr$ throughout Phanerozoic time. *Geology,* 10: 516-519.

Claypool, G.E., Holser, W.T., Kaplan, I.R., Sakai, H. and Zak, I. (1980): The age curves of sulfur and oxygen isotopes in marine sulfate and their mutual interpretation. *Chemical Geology,* 28: 199-260.

Cortecci, G., Reyes, E., Berti, G. and Casati, P. (1981): Sulfur and oxygen isotopes in Italian marine sulfates of Permian and Triassic ages. *Chemical Geology,* 34: 65-79.

Fanlo, I. and Ayora, C. (1998): The evolution of the Lorraine evaporite basin: Implications for the chemical and isotope compositions of the Triassic ocean. *Chemical Geology,* 146: 135-154.

Flügel E., Flügel-Kahler E., Martin, J.M. and Martín-Algarra, A. (1984): Middle Triassic reefs from Southern Spain. *Facies,* 11: 173-218.

García-Veigas, J., Cendón, D.I., Rosell, L., Ortí, F., Torres Ruiz, J., Martín, J.M. and Sanz, E. (2013): Salt deposition and brine evolution in the Granada Basin (Late Tortonian, SE Spain). *Palaeogeography, Palaeoclimatology and Palaeoecology,* 369: 452-465.

Gibert, L., Ortí, F. and Rosell, L. (2007): Plio-Pleistocene lacustrine evaporites of the Baza Basin (Betic Chain, SE Spain). *Sedimentary Geology,* 200: 89-116.

Gómez, J.J. and Goy, A. (1998): Las unidades litoestratigráficas del tránsito Triásico-Jurásico en la región de Lécera (Zaragoza). *Geogaceta,* 23: 63-66.

Gómez-Alday, J.J., Castaño, S. and Sanz, D. (2004): Origen geológico de los contaminantes (sulfatos) presentes en las aguas subterráneas de la Laguna de Petróla (Albacete, España). Resultados preliminares. *Geogaceta,* 35: 167-170.

Holland, H.D. (1984): *The Chemical Evolution of the Atmospheres and Ocean*. Princeton University, Princeton N.J., 583 p.

Iribar, V. and Ábalos, B. (2011): The geochemical and isotopic record of evaporite recycling in spas and salterns of the Basque Cantabrian basin, Spain. *Applied Geochemistry,* 26: 1315-1329.

Korte, Ch., Kozur, H.W., Bruckschen, P. and Veizer, J. (2003): Strontium isotope evolution of Late Permian and Triassic seawater. *Geochimica et Cosmochimica Acta,* 67: 47-62.

Longinelli, A. and Flora, O. (2007): Isotopic composition of gypsum samples of Permian and Triassic age from north-eastern Italian Alps: Paleoenvironmental implications. *Chemical Geology,* 245: 275-284.

Martín-Algarra, A, Solé de Porta, N. and Márquez-Aliaga, A. (1995): Nuevos datos sobre la estratigrafía, paleontología y procedencia paleogeográfica del Triásico de las escamas del Corredor del Boyar (Cordillera Bética Occidental). *Cuadernos de Geología Ibérica,* 19: 279-307.

McArthur, J.M., Howarth, R.J. and Bailey, T.R. (2001): Strontium isotope stratigraphy: LOWESS version3: best fit to the marine Sr-isotope curve for 0-509 Ma and accompanying look-up table for deriving numerical age. *Journal of Geology,* 109: 155-170.

Moragas, M., Playà, E., Rosell, L. and Inglès, M. (2011): Sedimentary and diagenetic processes in the Las Minas de Hellín Gypsum Unit (Upper Miocene, SE Spain). In: *Abstracts, 28th IAS Meeting of Sedimentology*, Zaragoza, Spain (Eds. B. Bádenas, M. Aurell and A.M. Alonso-Zarza), 61.

Ortí, F. (1987): Aspectos sedimentológicos de las evaporitas del Triásico y del Liásico Inferior en el E de la Península Ibérica. *Cuadernos de Geología Ibérica,* 11: 837-858.

Ortí, F. and Pueyo, J.J. (1983): Origen marino de la sal triásica del domo de Pinoso (Alicante, España). *Acta Geológica Hispánica,* 18: 139-145.

Ortí, F., Rosell, L. and Salvany J.M. (1992): Depósitos evaporíticos en España: Aspectos geológicos y recursos. In: *Recursos Minerales de España* (J. García Guinea and J. Martínez Frías, coord.). Textos Universitarios, 15, CSIC, 1171-1209.

Ortí, F., García-Veigas, J., Rosell, L., Jurado, MªJ. and Utrilla, R. (1996): Formaciones salinas de las cuencas triásicas en la Península Ibérica: caracterización petrológica y geoquímica. *Cuadernos Geologia Ibérica*, 20: 13-35.

Pérez-López, A. (1998): Epicontinental Triassic of the Southern Iberian Continental Margin (Betic Cordillera, Spain). In: *Epicontinental Triassic* (G.H., Bachmann and I. Lerche, Eds.), E. Schweizerbart'sche Verlagsbuchhandlung, Stuttgart, 1009–1031.

Pérez-López, A. and Pérez-Valera, F. (2003): El diapirismo como factor principal de la resedimentación de las rocas del Triásico durante el Terciario en las Zonas Externas de la Cordillera Bética. *Geotemas,* 5: 189-193.

Pérez-López, A. and Pérez-Valera, F. (2007): Palaeogeography, facies and nomenclature of the Triassic units in the different domains of the Betic Cordillera (S Spain). *Palaeogeography, Palaeoclimatology and Palaeoecology,* 254: 606-626.

Pérez-López, A. and Pérez-Valera, F. (2012): Tempestite facies models for the epicontinental Triassic carbonates of the Betic Cordillera (S Spain). *Sedimentology,* 59: 646-678.

Pérez-López, A., Pérez-Valera, F. and Götz, A. (2012): Record of epicontinental platform evolution and volcanic activity during a major rifting phase: The Late Triassic Zamoranos Formation (Betic Cordillera, S Spain). *Sedimentary Geology,* 247-248: 39-57.

Pérez-Valera, F. and Pérez-López, A. (2008): Stratigraphy and sedimentology of Muschelkalk carbonates of the Southern Iberian Continental Palaeomargin (Siles and Cehegín Formations, Southern Spain). *Facies,* 54: 61-87.

Pérez-Valera F, Solé de Porta N. and Pérez-López A. (2000): Presencia de facies Buntsandstein (Anisiense-Ladiniense?) en el Triásico de Calasparra (Murcia). *Geotemas,* 1: 209−211.

Playà, E., Ortí, F. and Rosell, L. (2000): Marine to non-marine sedimentation in the upper Miocene evaporites of the Eastern Betics, SE Spain: sedimentological and geochemical evidence. *Sedimentary Geology*, 133: 135-166.

Rick, B. (1990): Sulphur and oxygen isotope composition of Swiss Gipskeuper (Upper Triassic). *Chemical Geology,* 80: 243-250.

Utrilla, R., Pierre, C., Ortí, F. and Pueyo, J.J. (1992): Oxygen and sulfur isotope composition as indicators of the origin of Mesozoic and Cenozoic evaporites from Spain. *Chemical Geology,* 102: 229-244.

Veizer, J., Ala, D., Azmy, K., Bruckschen, P., Buhl, D., Bruhn, F., Garden, G.A.F., Diener, A., Ebneth, S., Dodderis, Y., Asper, T., Korte, Ch., Pawellek, F., Podlaha, G. and Strauss, H. (1999): $^{87}Sr/^{86}Sr$ and $\delta^{18}O$ evolution of Phanerozoic seawater. *Chemical Geology,* 161: 59-88.

Vera, J.A. (2004): Cordillera Bética y Baleares. In: *Geología de España* (J.A. Vera, Ed.), SGE-IGME, Madrid, 347-464.

Wortmann, U.G. and Paytan, A. (2012): Rapid Variability of Seawater Chemistry Over the Past 130 Million Years. *Science,* 337: 334-336.

Manuscrito recibido el 16-10-2013
Recibida la revisión el 29-01-2014
Aceptado el manuscrito revisado el 7-02-2014